



# 1 Multi-scenario urban flood risk assessment by integrating future 2 land use change models and hydrodynamic models

3 Qinke Sun<sup>1,2</sup>, Jiayi Fang<sup>1,2</sup>, Xuewei Dang<sup>3</sup>, Kepeng Xu<sup>1,2</sup>, Yongqiang Fang<sup>1,2</sup>, Xia Li<sup>1,2</sup>, Min Liu<sup>1,2</sup>

4 <sup>1</sup>School of Geographic Sciences, East China Normal University, Shanghai 200241, China

5 <sup>2</sup>Key Laboratory of Geographic Information Science (Ministry of Education), East China Normal University, Shanghai  
6 200241, China

7 <sup>3</sup>Faculty of Geomatics, Lanzhou Jiaotong University, Lanzhou 730070, China

8

9 *Correspondence to:* Jiayi Fang (jyfang822@foxmail.com); Min Liu (mliu@geo.ecnu.edu.cn)

10 **Abstract.** Urbanization and climate change are the critical challenges in the 21<sup>st</sup> century. Flooding by extreme weather  
11 events and human activities can lead to catastrophic impacts in fast-urbanizing areas. However, high uncertainty in climate  
12 change and future urban growth limit the ability of cities to adapt to flood risk. This study presents a multi-scenario risk  
13 assessment method that couples the future land use simulation model (FLUS) and floodplain inundation model (LISFLOOD-  
14 FP) to simulate and evaluate the impacts of future urban growth scenarios with flooding under climate change (two  
15 representative concentration pathways (RCPs 2.6 and 8.5)). By taking Shanghai coastal city as an example, we then quantify  
16 the role of urban planning policies in future urban development to compare urban development under multiple policy  
17 scenarios (Business as usual, BU; Growth as planned, GP; Growth as eco-constraints, GE). Geospatial databases related to  
18 anthropogenic flood protection facilities, land subsidence, and storm surge are developed and used as inputs to the  
19 LISFLOOD-FP model to estimate flood risk under various urbanization and climate change scenarios. The results show that  
20 urban growth under the three scenario models manifests significant differences in expansion trajectories, influenced by key  
21 factors such as infrastructure development and policy constraints. Comparing the urban inundation results for the RCP2.6  
22 and RCP8.5 scenarios, the urban inundation area under the GE scenario is less than that under the BU scenario, but more  
23 than that under the GP scenario. We also find that urban will tend to expand to areas vulnerable to floods under the  
24 restriction of ecological environment protection. The increasing flood risk information determined by the coupling model  
25 helps to understand the spatial distribution of future flood-prone urban areas and promote the re-formulation of urban  
26 planning in high-risk locations.

## 27 1 Introduction

28 Climate change and urbanization are the global challenges for the 21<sup>st</sup> century (Pecl et al., 2017; Ramaswami et al., 2016).  
29 Floods have been key threats for many cities around the world driven by global climate change (Fang et al., 2020; Hallegatte  
30 et al., 2013; IPCC, 2014). Currently, more than 600 million people worldwide live in the coastal cities that are less than 10 m



31 above sea level (United Nations, 2017a). The United Nations reports that the global population will increase by 29% (7.6  
32 billion) between 2017 and 2050 (United Nations, 2017b), which means that population of coastal cities will become  
33 increasingly concentrated in the future and impervious surfaces will become more numerous (Chen et al., 2020). On the  
34 other hand, the National Oceanic and Atmospheric Administration (NOAA) report suggests that global mean sea level will  
35 rise around 0.2 m to 2.0 m by 2100 under a continuing global warming trend (Parris et al., 2012). Additionally, properties  
36 and populations in many coastal areas will suffer more severely in the future if the effects of land subsidence are taken into  
37 account (Vousdoukas et al., 2018).

38 However, high uncertainty in flood risk and urban growth leads to a lack of capacity of cities to respond to the flooding  
39 arising from future climate change (Du et al., 2015; Fang et al., 2021; Tessler et al., 2015). Therefore, there is an urgent need  
40 for specialist knowledge and techniques to address the conflict between urbanization and flood risk (Bouwer, 2018; Haynes  
41 et al., 2018; Lai et al., 2016; Wang et al., 2015). For example, flood risk studies focus mainly on the current urban scenarios  
42 for disaster risk assessment (Bisht et al., 2016; Zhou et al., 2019); and partly consider future land use changes, but urban  
43 growth scenarios are mainly limited to original typologies (business-as-usual development) growth scenarios for study  
44 (Huong and Pathirana, 2013; Muis et al., 2015), with less consideration of environmental factors and urban growth scenarios  
45 under planning constraints (Lin et al., 2020; Long and Wu, 2016); thus, the lack of knowledge of future urban development  
46 scenarios leads to a lack of awareness of the consequences of future flooding (Kim and Newman, 2020; Zhao et al., 2017).  
47 On the other hand, the failure to integrate with broader climate change-related scenarios and possible extreme-case flood  
48 risks has led to underinvestment in climate adaptation actions by governments that do not well address the spatial  
49 consequences of future floods (Berke et al., 2019; Reckien et al., 2018). Thus, there is an urgent to adopt a more  
50 comprehensive approach that considers the complexity of multiple possible scenarios of urbanization and dynamic flood risk  
51 in an integrated manner.

52 This paper uses the coupling of the future land use simulation model (FLUS) and the 2D floodplain inundation model  
53 (LISFLOOD-FP) to explore the possible interaction between different urbanization development scenarios and climate  
54 change scenarios. The FLUS model improves the simulation accuracy of the model by combining artificial neural network  
55 (ANN) and Cellular automata (CA) model to simulate nonlinear land use changes while considering parameters related to  
56 environment, society, climate change, etc. (Liu et al., 2017; Zhai et al., 2020). The LISFLOOD-FP model has become a  
57 mature hydrodynamic model that can predict potential flood events in near real-time and are widely used in engineering  
58 applications (Sosa et al., 2020; Wing et al., 2019). The coastal metropolitan Area of Shanghai in the Yangtze River Delta in  
59 China, one of the fastest urbanizing cities in the world, is used as a case study.

60 The paper asks, how can combining different urban growth scenarios with climate change scenario analysis help inform  
61 preparedness for flood risks from climate change in urban flood risk assessments? To answer this question, we first consider  
62 how urban grow under different environmental and planning factors in the future. Secondly, we coupled urban growth and  
63 flood risk scenarios and compared them using climate change scenarios from two representative concentrated pathways  
64 (RCP 2.6 and 8.5) proposed by the Intergovernmental Panel on Climate Change (IPCC). The research illustrates the

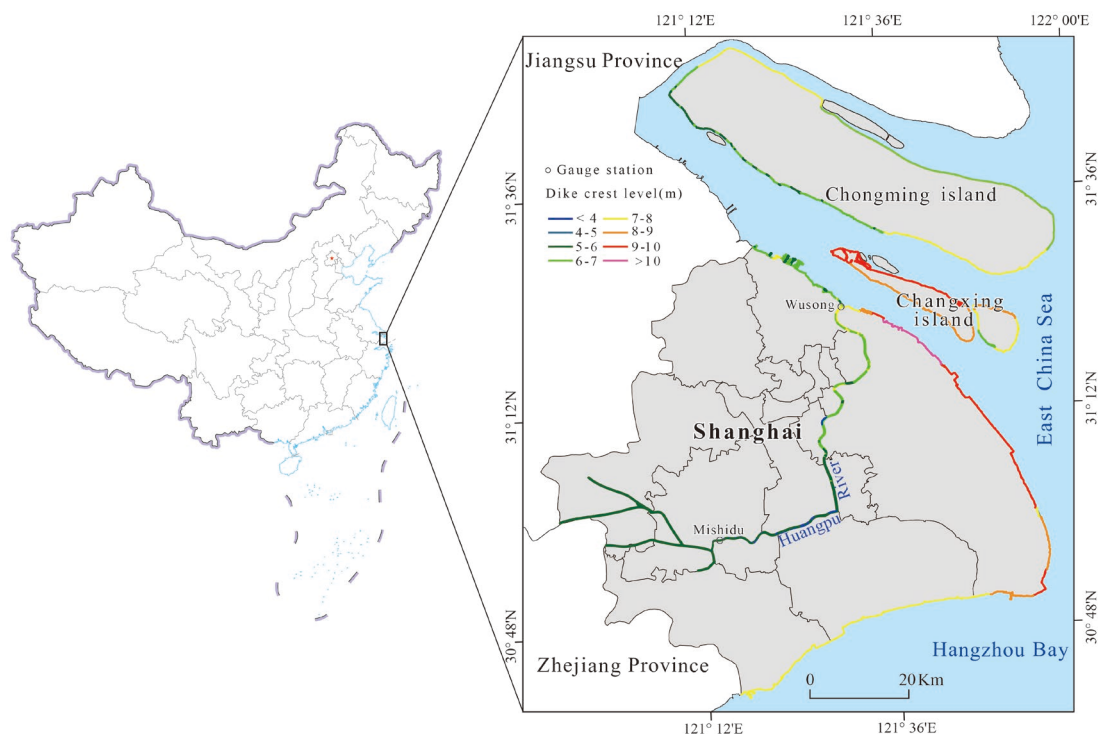


65 importance of assessing the performance of different future urban development scenarios in response to climate change, and  
66 the simulation study of urban risks will prove to decision-makers that incorporating disaster prevention measures into urban  
67 development plans will help reduce disaster losses and improve the ability of urban systems to respond to floods.

## 68 **2 Study area and datasets**

### 69 **2.1 Study area**

70 As the alluvial plain of the Yangtze River Delta, Shanghai is located on the coast of the East China Sea between 30°40'–  
71 31°53'N and 120°52'–122°12'E, which borders the provinces of Jiangsu and Zhejiang to the west. It's a typical middle  
72 latitude transition belt, marine land transitional zone and also a typical estuarine and coastal city with fragile ecological  
73 environment. The land area of Shanghai is about 6340.50 km<sup>2</sup>, accounting for 0.06 % of the total area of China, and has 213  
74 km of coastlines. The Shanghai metropolitan has undergone rapid urban expansion in the past decades and has become one  
75 of the largest urban areas in the world in both size and population(Sun et al., 2020). However, Shanghai's topography is low,  
76 with an average elevation of 4 m above sea level, and there is no natural barrier against storm surges. In 1905, one of the  
77 deadliest storm surges occurred in Shanghai, killing more than 29,000 people. Two years later, Typhoon Winnie made  
78 landfall in Shanghai, flooded more than 5,000 households (Du et al., 2020). Additionally, due to land subsidence and the  
79 increasing frequency and intensity of storm surge make Shanghai will become one of the most sensitive regions to the global  
80 climate change.



81  
82 **Figure 1: Location map of the study area. The main inland rivers in Shanghai flow into the East China Sea through the Huangpu**  
83 **River. The line with coloured vectors in the figure indicates the different dike crest level in Shanghai.**

## 84 2.2 Data

85 The research used three main categories of data, including basic data, scenarios constraints data and flood simulation data  
86 (Table 1). The basic data include land use, topography, traffic network, traffic site, socio-economic data. The land use data  
87 with a resolution of 100 m×100 m from the Resource and Environmental Science and Data Center of the Chinese Academy  
88 of Sciences is currently the most accurate land use remote sensing monitoring data product in China (Liu et al., 2014). The  
89 data for 2005 and 2010 were derived from Landsat-TM/ETM remote sensing image data respectively, and the data for 2015  
90 were interpreted using Landsat 8 remote sensing image. After the data was corrected and manually interpreted, the  
91 comprehensive evaluation accuracy of the interpretation accuracy of the first-class types of cultivated land, woodland,  
92 grassland, water area, urban land, and unused land reached more than 94.30%, and the discrimination accuracy rate on the  
93 map patches reached 98.70% (Xu et al., 2017). Within the allowable error range, it can be used as the basic data for  
94 analyzing land use changes.

95 Topography factors (DEM, slope), traffic network factors (distance to railway, highway, subway, and main roads), traffic  
96 site factors (distance to the city center, train station, and airports) and socio-economic factors (population, GDP), etc. as well  
97 as planning constraints, were determined to be spatial influence factors of the flood risk assessment of the Shanghai. The



98 Advanced Spaceborne Thermal Emission and Reflection Radiometer (ASTER) digital elevation model (DEM), which has  
 99 30-meter resolution, served as the basis data for terrain heights and slopes. Traffic network and site were collected from  
 100 open-source data retrieved from OpenStreetMap (OSM) and POI data were extracted from Tencent Map. Euclidean distance  
 101 was calculated for all vector data. The data of population and gross domestic product (GDP), were provided by the Resource  
 102 and Environmental Science and Data Center of the Chinese Academy of Sciences (Xu, 2017a, 2017b), and their time span  
 103 was consistent with the land use data. According to the simulation forecast demand, all materials were converted into  $100 \times$   
 104  $100$  m grid by resampling. The spatial limiting factors were the basic ecological control line, permanent basic cropland and  
 105 cultural protection control line as outlined in the 2017–2035 Shanghai City Master Plan. All the impact factor data were  
 106 normalized, and the range of the value is between 0 and 1 to subsequent data mining.  
 107 The storm surge data comes from the Global Tide and Surge Reanalysis (GTSR) dataset, which has been validation to have  
 108 good accuracy (Muis et al., 2016). In addition, man-made flood defenses have been considered to reasonably evaluate the  
 109 inundation impact of the flooding. The coastal flood protection data was obtained from the historical archival of the  
 110 Shanghai Water Authority for Shanghai (Yin et al., 2020). All data sources are listed in in the table below.

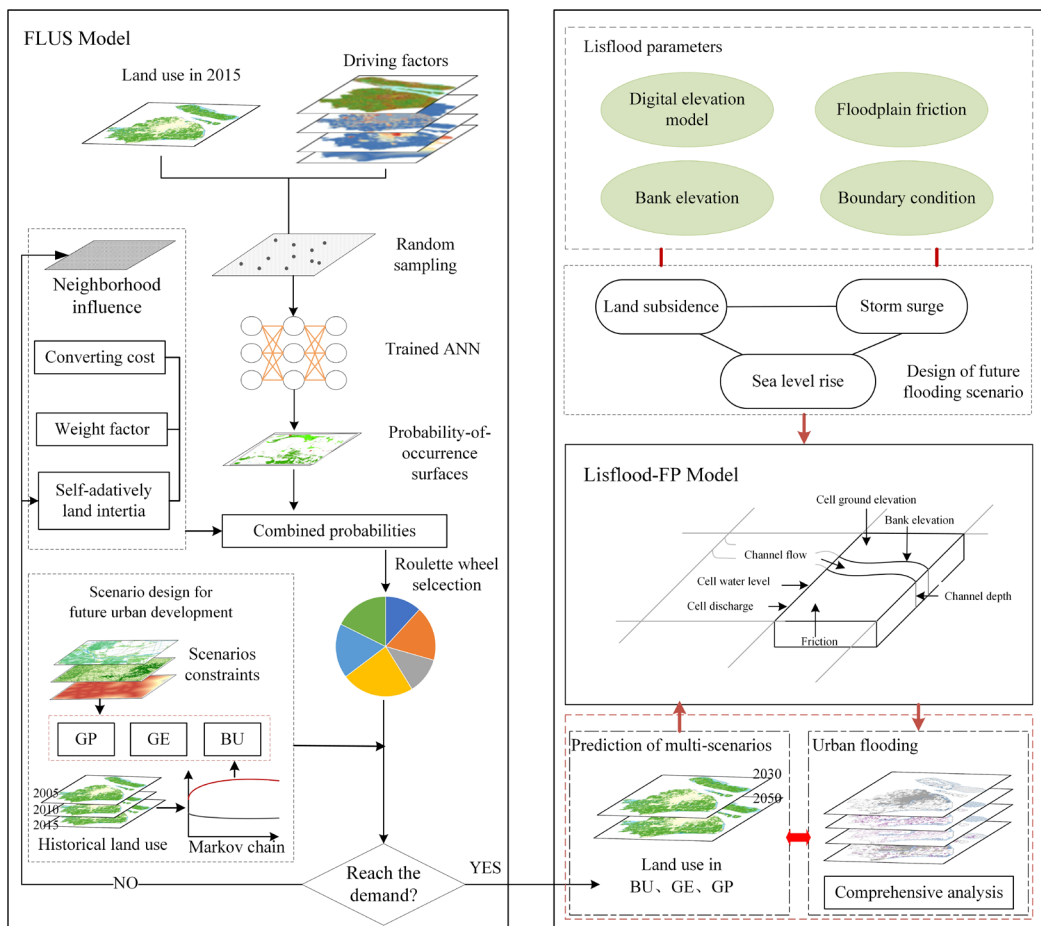
111 **Table 2. Data required and sources. The list details the resolution and sources of the data in the study.**

Category	Data Type	Resolution	Source
Basic data	Land use	$100 \text{ m} \times 100 \text{ m}$	Resource and Environmental Science and Data Center ( <a href="http://www.resdc.cn">http://www.resdc.cn</a> )
	Topography	Vector line	ASTER GDEM ( <a href="https://earthexplorer.usgs.gov/">https://earthexplorer.usgs.gov/</a> )
	Traffic network	Vector line	OpenStreetMap ( <a href="https://www.openstreetmap.org">https://www.openstreetmap.org</a> )
	Traffic site	Vector point	Tencent Map ( <a href="https://map.qq.com/">https://map.qq.com/</a> )
	Social economy	$1 \text{ km} \times 1 \text{ km}$	Resource and Environmental Science and Data Center
Scenarios constraints	Ecological control line	Vector line	《2017-2035 Shanghai City Master Plan》
	Permanent basic cropland control line	Vector line	
	Cultural protection control line	Vector line	
Flood data	Floodwalls	Vector line	Shanghai Water Authority ( <a href="http://swj.sh.gov.cn/">http://swj.sh.gov.cn/</a> )
	Storm surge	Vector line	GTSR



112 **3 Methodology**

113 The presented approach for relative sea level rise scenario flood risk assessment is the integration of the FLUS model,  
 114 LISFLOOD-FP model, and Markov chain model. In the framework, the FLUS model and Markov chain model are designed  
 115 to stimulate complexity land-use change processes in three different scenarios through 2030 to 2050, which include Business  
 116 as usual (BU), Growth as planned (GP), Growth as eco-constraints (GE) scenarios. A Markov chain model is used to predict  
 117 land-use demand in 2030 and 2050 combine planning policy factors, which is one of the crucial data inputs in the FLUS  
 118 model. Next, the LISFLOOD-FP two-dimensional flood model is used to explore the potential flooding areas under the RCP  
 119 2.6 and 8.5 scenarios in 2030 and 2050, to avoid the overestimation of the submerged range based on the GIS-based  
 120 elevation area method. This model also considers the compound influence of sea-level rise, storm surge, and land subsidence,  
 121 Finally, via ArcGIS spatial comprehensive analysis, the flooding of different land types is calculated employing different  
 122 flooding scenarios. The overall flow chart of research is illustrated in Fig. 2.



123  
 124 **Figure 2: The overall flow chart of research.**



### 125 3.1 Markov chain model

126 Markov chain model refers to the random transition process of state from one state to another, and its future state is only  
127 related to the state at previous moment. In the study of land use change, the type of land use at a certain moment is only  
128 related to the type of land use at the previous moment. Therefore, land-use change is a typical Markov process and has  
129 widely used in the prediction of land-use changes (Zhou et al., 2020). We predicted future land use by Eq. (1):

$$130 S_{(t+1)} = P_{i,j} \times S_t \quad (1)$$

131 where  $S_t$  and  $S_{t+1}$  represent the land use at times  $t$  and  $t+1$ , and  $P_{i,j}$  is a state transition matrix that land-use type  $i$  is  
132 converted to land-use type  $j$ . This model has a good predictive effect on the process state (Gounaridis et al., 2019). Therefore,  
133 we use the Markov chain to calculate the probability of the conversion of various land types, and then predict the number of  
134 future land change.

### 135 3.2 The FLUS land use simulation model

136 The FLUS model is an upgraded version of cellular automata model (Liu et al., 2017), which can solve the complex land  
137 use simulation problems by self-adaptive inertia and competition mechanism. The FLUS shows the highest current  
138 performances than other simulation models such as CLEU-S, SLEUTH, and LTM and has been applied to land use change  
139 simulation research at different scales and for different purposes (Liang et al., 2018; Lin et al., 2020).

140 As the most important scheme to manage the space of the urban, urban land use plan can reflect the general arrangement of  
141 land use in the future (Xu and Yang, 2019). In this research, three categories of urban growth scenarios are simulated  
142 through the FLUS model. The similarity of the three scenarios is that they use factors that affect urban development and  
143 changes, such as population, GDP, traffic, and slope, as the main spatial driving factors. The difference is as follows:

144 (i) Business as usual (BU): BU is natural growth without development laws and regulations. Its development is based on the  
145 premise of the current urban development patterns. Therefore, the land demand predicted by Markov is used as the constraint  
146 condition for the iteration of CA model in the subsequent application of the scenario.

147 (ii) Growth as planned (GP): Under the GP scenario, the urban growth projection that closely link to the master plan for  
148 Shanghai in terms of quantity, reflecting how the city government prefer to develop. The master plan requires that the total  
149 area of planned urban construction land does not exceed 3,200 km<sup>2</sup> in 2035. As the condition for the model iteration to stop,  
150 we estimated the urban area to be 2,768 km<sup>2</sup> in 2030 and 3,200 km<sup>2</sup> in 2050 combined with urban master plan.

151 (iii) Growth as eco-constraints (GE): The GE scenario is an eco-environmental protection scenario which development is  
152 limited by the ecological environment protection. Combined with Shanghai's ecological and environmental protection  
153 requirements and the distribution of permanent basic farmland, sensitive areas restricted for development are identified at the  
154 scenario, and we also establish a cultural protection control line for strengthening historical and cultural protection. In



155 addition, the number of areas of future urban growth in GE scenario also combines the requirements given in the urban  
156 master plan to enhance the reality of the scenario.

157 Therefore, the FLUS model is used to simulate future urban growth combines various scenarios. First, the driving factors and  
158 land-use data is trained by ANN model to obtain a probability-of-occurrence map, and then incorporate with the self-  
159 adaptive land inertial, conversion cost, and neighborhood competition among the different land use types to estimate the  
160 combined probability for each grid. Next, combining the number of various types of land predicted by the Markov Chain  
161 model and the constraints of each scenario to predicted urban growth in 2030 and 2050. To better validate the model before  
162 predicting for future change, we compared output to the actual land use 2015. Note that the number of iterations in each  
163 scenario is set to 5000, which is much higher than the default value to show higher prediction accuracy.

### 164 3.3 The LISFLOOD-FP flood inundation model

165 LISFLOOD-FP is a 2D hydraulic model based on a raster grid (Bates et al., 2010), which can efficiently simulate the  
166 dynamic propagation of flood waves over fluvial and estuarine floodplains and show real-time changes in water depth of  
167 complex terrain. LISFLOOD-FP model solves the Saint-Venant equations at very low computational cost by omitting only  
168 the convective acceleration term over a structured grid using a highly efficient explicit finite difference scheme to produce a  
169 two-dimensional simulation of floodplain hydrodynamics (O’Loughlin et al., 2020). The model has been widely used in the  
170 applications of small-scale and large-scale urban waterlogging and flooding.

171 In the present study, the LISFLOOD-FP model is used to simulate storm surge floods along the coast of Shanghai and floods  
172 along the Huangpu River. The effectiveness of the model in the study area has been verified by another article of our group  
173 members and shows good simulation results (Xu et al., 2021). In the boundary control of model, hydrological stations and  
174 global storm surge data are respectively employed as the input of the scenario design. However, Shanghai Geological  
175 Environmental Bulletin and land subsidence control plan show that land subsidence has a significant contribution to the  
176 flood hazards in Shanghai (Xian et al., 2018). With reference to the research of Yin et al (Yin et al., 2013), the values of land  
177 subsidence in 2030 and 2050 are selected to be 0.12 m and 0.24 m, respectively. This study also combines the storyline of  
178 future scenario of the IPCC, namely the Representative Concentration Pathway (RCP) scenarios, and selects conservative  
179 (RCP2.6) and largest magnitude (RCP8.5) climate-change scenarios, which values from Kopp et al (Kopp et al., 2017). For  
180 the simulation of the Huangpu River flood, we conducted experiments for 50-year return period under the RCP2.6 scenario  
181 and 100-year return period under the RCP8.5 scenario respectively during 2030 to 2050. For the 2030 and 2050, both  
182 Huangpu River and the coastal floods are followed to the RCP2.6 and RCP8.5 scenarios. Finally, we combine land  
183 subsidence and the RCP data to control the flood inundation simulation.

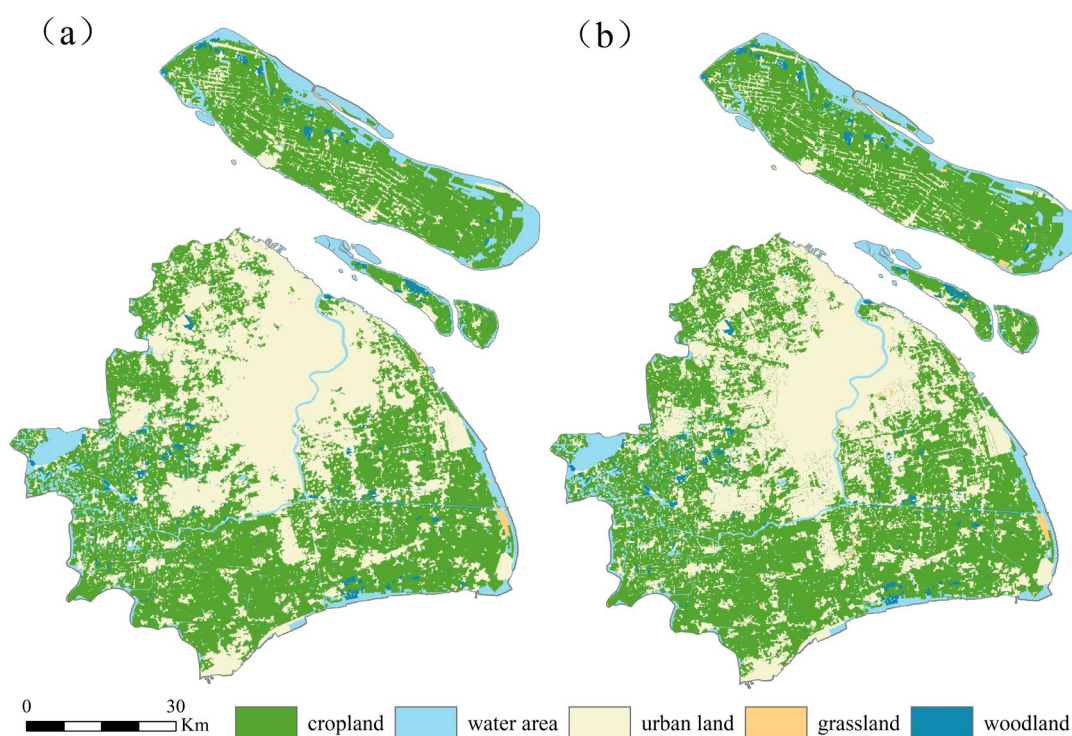




## 184 4 Results

### 185 4.1 Model validity

186 Model verification is the prerequisite for model operation, and the operation can only be carried out after confirming the  
187 model that is considered valid. The applicability of the proposed model was tested by simulating LUCCs in 2015 at Shanghai.  
188 The spatial simulation result shows that the simulated result and the actual land use have a high consistency (Fig. 3). We  
189 compared the actual land use and the simulated result pixel by pixel in our study and found the overall accuracy (OA) was  
190 93.20%, the kappa coefficient (kappa) was 0.89. The discrepancy of the actual land use and simulated result is likely due to  
191 the neighborhood interaction in the CA model, in which grid cells in more urbanized neighborhoods have a higher  
192 probability to convert to urban, whereas the grid cells are less likely to change to urban in less urbanized neighborhoods.  
193 Overall, the model accuracy outputs are measured shows an acceptable or good level of prediction, therefore the model is  
194 suitable for predicting changes in land use of Shanghai.



195

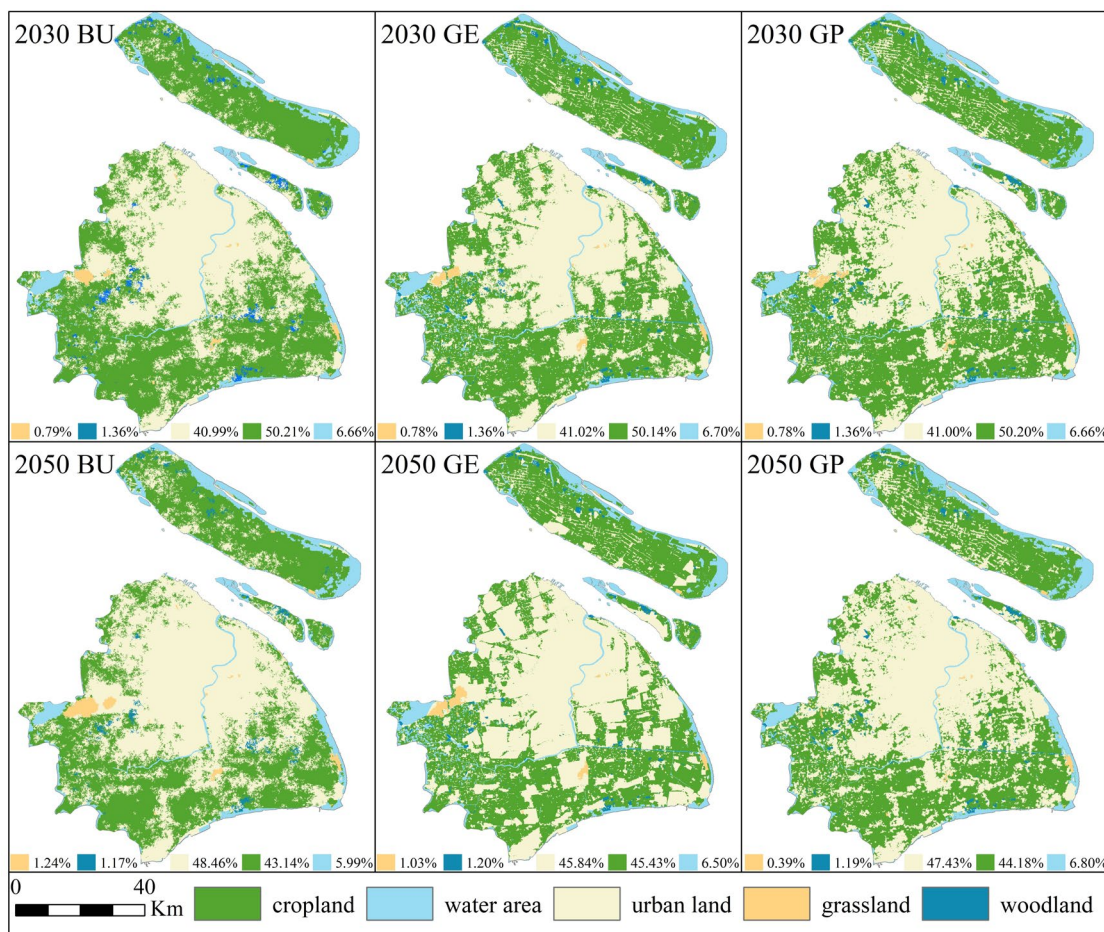
196 **Figure 3: Comparing the simulation results of Shanghai urban expansion with the actual situation, (a) simulation result in 2015; (b)**  
197 **actual land use in 2015.**



## 198 4.2 Future land use changes

199 Based on the conditions under three different development scenarios, we predicted the development of future urban land use  
200 change in 2030 and 2050. The prediction result shows different development patterns for each scenario (Fig. 4). Future urban  
201 growth under the BU scenario is primarily located in northwestern with some development in the central regions, and under  
202 the GP scenario the urban growth involves evenly distributed development. Urban growth in the GE scenario, however,  
203 Chongming Island regions have seen more urban growth, and the downtown area is not fully occupied by urban expansion  
204 due to restrictions.

205 Due to the impact of infrastructure construction, distance to the city center, and policy restrictions, Shanghai's overall urban  
206 expansion model shows a center-peripheral expansion. The built-up land areas in 2030 and 2050 are respectively project to  
207 increase by about 6 % and 13 % as compare to 2015, the most significant reduction is found for cultivated land and  
208 woodland. Specifically, the built-up land areas in 2030 are respectively project to increase by 427.32 km<sup>2</sup>, 428.27 km<sup>2</sup> and  
209 429.12 km<sup>2</sup> at BU, GP and GE scenarios, the built-up land areas in 2050 are respectively project to increase by 926.38 km<sup>2</sup>,  
210 857.63 km<sup>2</sup> and 751.47 km<sup>2</sup> at BU, GP and GE scenarios. The most significant reduction is found for cropland, which is  
211 predicting in 2050 to decrease by 876.97 km<sup>2</sup>, 857.63 km<sup>2</sup> and 723.59 km<sup>2</sup> as compared to 2015 in BU, GP and GE scenarios.  
212 The southwestern region is not suitable for large-scale urban development, due to large amounts of farmland in the region  
213 are listed as ecological protection areas, so the slow growth of these areas is not expected. The simulation maps show, as  
214 expected, land use changes under different planning scenarios, especially the urban sprawl trend at the GE scenario, creating  
215 new development areas in suburbs. To sum up, the urban expansion trajectory under BU, GP and GE shows significant  
216 differences, and these changes mainly at the expense of the cropland.



217  
 218 **Figure 4: Simulation results of different scenarios in 2030 and 2050. Each image shows the spatial distribution and the proportion**  
 219 **of area of different land use types in the simulated scenario.**

220 **4.3 Changing flood hazard in the future**

221 The LISFLOOD-FP model is used to simulate the flood evolution process under RCP2.6 and RCP8.5 scenarios (the  
 222 inundation results are plotted in Supplementary Figure 1), and then the submerged depth and area under different scenarios  
 223 are statistically analyzed to explore the future flood risk under different RCP scenarios. First, the maximum water depth risk  
 224 of the submerged area is counted, and the submerged area is divided into four depth levels: the submerged water depth is less  
 225 than 0.5 m as shallow water area, water depth is 0.5-1 m as medium water area, the water depth is 1-2 m as deep water area,  
 226 and submerged water depth is above 2 m as the extremely deep area. The area and proportion of each water depth level are  
 227 calculated.

228 By comparing the scenarios in RCP2.6 and RCP8.5, it is evident that the submerged area increasing trends with time (Table  
 229 2). The total flooded area increased by 162.43 km<sup>2</sup> and 189.44 km<sup>2</sup> under RCP2.6 and RCP8.5 scenarios from 2030 to 2050,



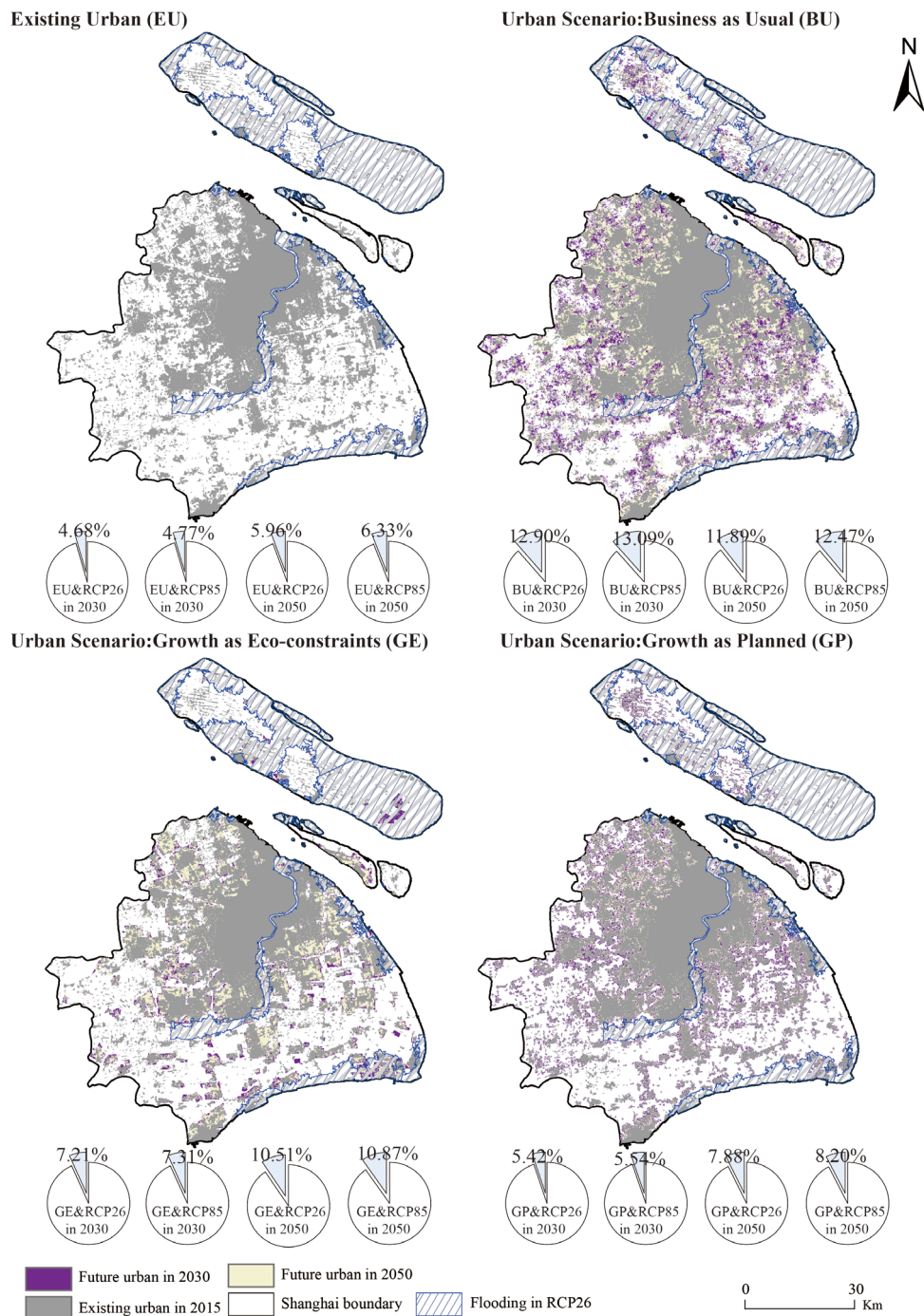
230 respectively. Additionally, the depth of submergence and the extent of submergence will gradually increase as the floodwater  
 231 spreads. Taking the area with submergence depth above 2 m as an example, under RCP2.6 scenario the area with  
 232 submergence is 353.69 km<sup>2</sup> and 401.57 km<sup>2</sup> respectively in 2030 and 2050, and under RCP8.5 scenario the area with  
 233 submergence is 356.28 km<sup>2</sup> and 418.36 km<sup>2</sup> respectively in 2030 and 2050. It shows that Shanghai will still face great flood  
 234 risk under these two scenarios.

235 **Table 2. Statistics of flood water depth.**

Category	<0.5 m		0.5-1 m		1-2 m		>2 m		Total /km <sup>2</sup>
	Area/ km <sup>2</sup>	Ratio/ %	Area/ km <sup>2</sup>	Ratio/ %	Area/ km <sup>2</sup>	Ratio/ %	Area/ km <sup>2</sup>	Ratio/ %	
2030 RCP2.6	138.61	14.54	164.07	17.21	296.98	31.15	353.69	37.10	953.35
2030 RCP8.5	137.13	14.23	169.76	17.61	300.82	31.21	356.28	36.96	963.99
2050 RCP2.6	125.04	11.21	229.81	20.60	359.36	32.21	401.57	35.99	1115.78
2050 RCP8.5	141.72	12.29	219.58	19.04	373.77	32.41	418.36	36.27	1153.43

236 **4.4 Future changes in urban flood risk**

237 The flood risk of the urban is calculated by overlapping existing urban and projected future urban scenarios with future flood  
 238 risk zones. First, in the existing urban exposure to future flood risk scenarios (the upper left in Fig. 5), more urban areas will  
 239 be vulnerable to flood risk in the context of global climate change. Under the RCP 2.6 scenario, 4.68 % and 5.96 % of the  
 240 total existing urban areas in 2030 and 2050 would be susceptible to flood risk, respectively. In the 2030 and 2050 of the  
 241 RCP8.5 scenarios the area of existing urban land which would be vulnerable to future flood risks are 110.27 km<sup>2</sup> and 146.23  
 242 km<sup>2</sup>, respectively. Many urban areas will be flooded under sea level rise caused by climate change even when protected by  
 243 levees, and more than 5% of urban areas in Shanghai are still in the floodplain.



244

245 **Figure 5: Flood exposure of existing urban and future urban growth scenarios. The four pie charts for the BU, GE, and GP**  
 246 **scenarios represent the proportion of new growth urban area exposed to flooding under the 2030RCP2.6, 2030RCP8.5,**  
 247 **2050RCP2.6, and 2050RCP8.5, respectively. The four pie charts for the EU scenarios represent the proportion of the existing**  
 248 **urban area affected by the future flood risk scenario.**



249 Future urban development would occur in the flood zone, with the rapid expansion of the urban. Fig. 5 also shows the  
 250 comprehensive analysis results of the three urban growth scenarios under different climate change scenarios. Under the  
 251 RCP2.6 scenario, new growth in urban land area affected by flooding in 2030 are respectively 55.11 km<sup>2</sup>, 23.22 km<sup>2</sup>, and  
 252 30.92 km<sup>2</sup> at BU, GP and GE scenarios. Under the RCP8.5 scenario, future more urban growth areas would be affected by  
 253 the flooding, which will be reached 12.47 %, 10.87 %, and 8.20 % at BU, GP and GE scenarios in 2050, respectively. In  
 254 general, the higher the sea level rises, the greater the risk of flooding in future urban areas. Small changes in sea level rise  
 255 will affect a large amount of land, due to the average altitude of Shanghai is around 4 m.  
 256 **Table 3. Inundate of each land use type under different scenarios. The inundated areas of different land use types, including**  
 257 **cropland, woodland, grassland and urban land, were calculated for each scenario, where <sup>a</sup> indicates new growth area of urban**  
 258 **affected by flooding.**

Time	Category	Urban scenario	Inundated areas (km <sup>2</sup> )			
			Cropland	Woodland	Grassland	Urban land <sup>a</sup>
2030	RCP2.6	BU	595.05	10.05	5.60	55.11
		GE	618.95	12.12	5.84	30.92
		GP	597.71	12.40	5.91	23.22
	RCP8.5	BU	602.38	10.23	5.67	55.92
		GE	625.97	12.29	5.91	31.23
		GP	604.32	12.59	5.98	23.72
2050	RCP2.6	BU	662.64	13.56	5.25	110.19
		GE	677.59	16.74	5.95	78.95
		GP	651.24	15.66	5.46	67.55
	RCP8.5	BU	683.56	15.06	5.70	115.53
		GE	698.98	18.05	6.40	81.71
		GP	672.30	16.85	5.91	70.36

259  
 260 The research found that the cultivated land is most affected by flooding (Table 3), and urban areas and woodland are the  
 261 second most affected. Under the GE scenario, the flooded area of cultivated land is 618.95 km<sup>2</sup> and 625.97 km<sup>2</sup> at the  
 262 RCP2.6 and RCP8.5 in 2030, and 677.59 km<sup>2</sup> and 698.98 km<sup>2</sup> at the RCP2.6 and RCP8.5 in 2050. Further, the exposure of  
 263 various types of land is increasing with time, but urban land and cropland will be the most impacted land types in the future.  
 264 Comparing the three scenarios we can find that the urban development area under the planning scenario is less affected by



265 flooding, as compared to the business-as-usual development scenario. Comparing the inundation of the two planning  
266 scenarios (GE and GP), also reflects the decision-makers' trade-off between economic development and ecological  
267 protection. The inundation area of the urban land under the GP scenario is less than that of the GE, which means that under  
268 the planning constraint of protecting ecological and cultural areas, urban built-up areas will develop on low-protection areas,  
269 which are more vulnerable to flooding. In conclusion, from reducing the risk of future flooding in urban areas, GE scenario  
270 shows to be better than BU scenario, but worse than GP scenario.

## 271 **5 Discussions**

### 272 **5.1 Source of uncertainties**

273 There are some limitations in our study, which is what we need to improve in the future. First, there is still more room to  
274 improve the accuracy of model prediction. In this study, the performance of the FLUS model is tested by kappa and OA  
275 measures, which shows a good range of prediction accuracy. In addition, this study proves that 16 driving factors contribute  
276 to the simulation and prediction of urban growth in Shanghai. The relationship between human and natural driving factors  
277 and land use change can be effectively integrated through the FLUS model embedded with an ANN, to obtain more realistic  
278 simulation results. However, if more influential drivers and the latest land cover are employed, the prediction would be  
279 having higher accuracy. Second, future flood risks in coastal areas also are not fully reflected through using of hydrodynamic  
280 models, although it shows higher accuracy than the elevation area submergence method. On the one hand, this study is based  
281 on the modeling results of DEM data, which may overestimate or underestimate the simulation effect due to the error of  
282 DEM data. On the other hand, extreme storm surge and land subsidence data are combined to enhance the reliability of the  
283 extreme flood forecast in this study. However, the change of the impervious surface that affects hydrology not be considered  
284 in this study. When other land uses are converted to urban land uses, the risk of flooding will also greatly increase due to  
285 changes the impervious surfaces. Therefore, it is necessary to dynamically adjust relevant factors affecting flood peak flows  
286 and risk in future forecasts to enhance the accuracy of prediction.

287 In the context of global climate change, extreme weather in the future may become more and more serious, so it is necessary  
288 to dynamically combine climate scenarios to develop more accurate flood risk delineation methods to guide urban planning  
289 in the future, and rely on new technology and equipment to provide data support, For example, unmanned aviation vehicles  
290 (UAVs) are deployed around the coastline to generate real-time information about weather conditions and sea-level changes  
291 (Cochrane et al., 2017). These tools will as a complement to existing information and early warning systems, which also can  
292 provide guidance for coastal flood risk management and urban planning in the future. Overall, although uncertainty cannot  
293 be avoided when assessing coastal flood risk, the deviation of the proposed model output is within an acceptable range,  
294 which ensures the accuracy of coastal flood risk assessments.



## 295 **5.2 Recommendations on strategies and policies for urban adaptation to flooding**

296 In the twenty-first century, adapting to climate change and coastal flooding is a critical challenge for coastal cities. Human  
297 response to the impacts of flooding largely depends on the allocation of urban facilities and managers' planning for future  
298 urban development (Hunt and Watkiss, 2011). Shanghai is considered one of the most protected Chinese cities in terms of  
299 flood protection, yet it's the EAD/GDP (the Expected Annual Disruption, EAD), that is the direct damage to buildings and  
300 vehicles) ratio is as much as five times than in New York (Aerts et al., 2014). Therefore, there is an urgent need to adopt  
301 flood risk adaptation strategies in Shanghai.

302 We conducted a set of comparative experiments to analyze the coastal flood damage in Shanghai with and without flood  
303 walls (hard adaptation strategies). Our analysis considered the important effects of land subsidence and SLR on flood risk.  
304 We found that the current flood protection wall can reduce the flood losses due to climate change to a relatively low level  
305 (Supplementary Figure 2). In comparison, the flood protection wall constructed for the current conditions would reduce the  
306 flooded area under the RCP8.5 scenario by about 35% and 36% in 2030 and 2050, respectively. This result shows that the  
307 current hard protection strategy can reduce the flood risk to a low level, but the residual flood risk from using the hard  
308 protection strategies still needs to be addressed. From the cases of advanced flood risk management countries such as the  
309 Netherlands (Kabat et al., 2009; Song et al., 2018), an important success lesson for future flood protection design is to leave  
310 enough space along coasts for wetland migration and leave space for nature. In other words, "soft strategies" such as  
311 "working with rivers and nature" are considered in the flood protection measures. Therefore, it is necessary to learn from the  
312 practical experience of advanced countries to strengthen the development and construction of coastal wetlands and tidal flat  
313 ecosystems, and further reduce the residual risk through the adaptive regulation of coastal ecosystems and other soft  
314 strategies. In addition, the implementation of "soft strategies" can increase the value of ecosystem services, increase  
315 biodiversity and carbon sequestration, and improve social welfare (Du et al., 2020).

## 316 **6 Conclusion**

317 Scenario-based assessment has been found to be a powerful approach in numerous flood risk studies. This study combines an  
318 urban growth model with a two-dimensional flood inundation model to not only simulate urban development dynamics more  
319 accurately, but also to discard the shortcomings of the traditional elevation inundation method of overestimating inundation  
320 areas. We have also tested the resilience of Shanghai to future different climate scenarios with current flood wall. The results  
321 of the study are beneficial to local planners and coastal managers in making decisions of future protected areas and  
322 developments.

323 This study employed three urban development scenarios and detected the relationships of urbanization and climate changes  
324 in 2030 and 2050. The results of the study show that urban growth under the three scenario models manifests significant  
325 differences in expansion trajectories, influenced by key factors such as infrastructure development and policy constraints.  
326 According to the predicted results of flood, new built-up areas are also potentially vulnerable areas of flood risk. New built-





327 up areas under different scenarios show significant vulnerability and exposure risk under different climate scenarios, even  
328 with the support of flood bank and other hard structures. Additionally, the research provided significant insights into the  
329 range and spatial distribution of flood risk in future urban.

330 The current study is based on the multi scenario analysis of RCP scenarios. In the future, the shared socioeconomic pathways  
331 (SSPs) can be combined to predict land use change, which make urban development scenarios have more realistic choices.  
332 The results of this study estimate the future urban flood exposure areas, but this does not mean that all flood-vulnerable areas  
333 will be flooded, only that in these areas, the probability of each possible occurrence is greater. Therefore, proper preparations  
334 (such as definition restricted development zones) can reduce the damage risk of future flood and build more resilient cities.

### 335 **Author contributions**

336 Q. Sun and J. Fang designed the research; Q. Sun, K. Xu and X. Dang collected the data and carried out the experiments; Q.  
337 Sun wrote the draft; J. Fang, X. Dang, Y. Fang and M. Liu revised the manuscript; J. Fang, X. Li and M. Liu supervised and  
338 provided critical feedback. All authors contributed to the final version of the manuscript.

### 339 **Competing interests**

340 The authors declare that they have no conflict of interest.

### 341 **Funding source**

342 This work was supported by a grant from the National Natural Science Foundation of China (No.42001096); Shanghai  
343 Sailing Program (19YF1413700); China Postdoctoral Science Foundation (No. 2019M651429).

### 344 **References**

- 345 Aerts, J. C. J. H., Botzen, W. J. W., Emanuel, K., Lin, N., De Moel, H. and Michel-Kerjan, E. O.: Climate adaptation:  
346 Evaluating flood resilience strategies for coastal megacities, *Science* (80-. ), 344(6183), 473–475,  
347 doi:10.1126/science.1248222, 2014.
- 348 Bates, P. D., Horritt, M. S. and Fewtrell, T. J.: A simple inertial formulation of the shallow water equations for efficient two-  
349 dimensional flood inundation modelling, *J. Hydrol.*, 387(1–2), 33–45, doi:10.1016/j.jhydrol.2010.03.027, 2010.
- 350 Berke, P. R., Malecha, M. L., Yu, S., Lee, J. and Masterson, J. H.: Plan integration for resilience scorecard: evaluating  
351 networks of plans in six US coastal cities, *J. Environ. Plan. Manag.*, 62(5), 901–920,  
352 doi:10.1080/09640568.2018.1453354, 2019.



- 353 Bisht, D. S., Chatterjee, C., Kalakoti, S., Upadhyay, P., Sahoo, M. and Panda, A.: Modeling urban floods and drainage using  
354 SWMM and MIKE URBAN: a case study, *Nat. Hazards*, 84(2), 749–776, doi:10.1007/s11069-016-2455-1, 2016.
- 355 Bouwer, L. M.: Next-generation coastal risk models, *Nat. Clim. Chang.*, 8(9), 765–766, doi:10.1038/s41558-018-0262-2,  
356 2018.
- 357 Chen, G., Li, X., Liu, X., Chen, Y., Liang, X., Leng, J., Xu, X., Liao, W., Qiu, Y., Wu, Q. and Huang, K.: Global projections  
358 of future urban land expansion under shared socioeconomic pathways, *Nat. Commun.*, 11(1), 537, doi:10.1038/s41467-  
359 020-14386-x, 2020.
- 360 Cochrane, L., Cundill, G., Ludi, E., New, M., Nicholls, R. J., Wester, P., Cantin, B., Murali, K. S., Leone, M., Kituyi, E. and  
361 Landry, M. E.: A reflection on collaborative adaptation research in Africa and Asia, *Reg. Environ. Chang.*, 17(5), 1553–  
362 1561, doi:10.1007/s10113-017-1140-6, 2017.
- 363 Du, S., Van Rompaey, A., Shi, P. and Wang, J.: A dual effect of urban expansion on flood risk in the Pearl River Delta  
364 (China) revealed by land-use scenarios and direct runoff simulation, *Nat. Hazards*, 77(1), 111–128,  
365 doi:10.1007/s11069-014-1583-8, 2015.
- 366 Du, S., Scussolini, P., Ward, P. J., Zhang, M., Wen, J., Wang, L., Koks, E., Diaz-Loaiza, A., Gao, J., Ke, Q. and Aerts, J. C.  
367 J. H.: Hard or soft flood adaptation? Advantages of a hybrid strategy for Shanghai, *Glob. Environ. Chang.*, 61, 102037,  
368 doi:https://doi.org/10.1016/j.gloenvcha.2020.102037, 2020.
- 369 Fang, J., Lincke, D., Brown, S., Nicholls, R. J., Wolff, C., Merkens, J. L., Hinkel, J., Vafeidis, A. T., Shi, P. and Liu, M.:  
370 Coastal flood risks in China through the 21st century – An application of DIVA, *Sci. Total Environ.*, 704, 135311,  
371 doi:10.1016/j.scitotenv.2019.135311, 2020.
- 372 Fang, J., Wahl, T., Zhang, Q., Muis, S., Hu, P., Fang, J., Du, S., Dou, T. and Shi, P.: Extreme sea levels along coastal China:  
373 uncertainties and implications, *Stoch. Environ. Res. Risk Assess.*, 35(2), 405–418, doi:10.1007/s00477-020-01964-0,  
374 2021.
- 375 Gounaridis, D., Choriantopoulos, I., Symeonakis, E. and Koukoulas, S.: A Random Forest-Cellular Automata modelling  
376 approach to explore future land use/cover change in Attica (Greece), under different socio-economic realities and scales,  
377 *Sci. Total Environ.*, 646, 320–335, doi:10.1016/j.scitotenv.2018.07.302, 2019.
- 378 Hallegatte, S., Green, C., Nicholls, R. J. and Corfee-Morlot, J.: Future flood losses in major coastal cities, *Nat. Clim. Chang.*,  
379 3(9), 802–806, doi:10.1038/nclimate1979, 2013.
- 380 Haynes, P., Hehl-Lange, S. and Lange, E.: Mobile Augmented Reality for Flood Visualisation, *Environ. Model. Softw.*, 109,  
381 380–389, doi:10.1016/j.envsoft.2018.05.012, 2018.
- 382 Hunt, A. and Watkiss, P.: Climate change impacts and adaptation in cities: A review of the literature, *Clim. Change*, 104(1),  
383 13–49, doi:10.1007/s10584-010-9975-6, 2011.
- 384 Huong, H. T. L. and Pathirana, A.: Urbanization and climate change impacts on future urban flooding in Can Tho city,  
385 Vietnam, *Hydrol. Earth Syst. Sci.*, 17(1), 379–394, doi:10.5194/hess-17-379-2013, 2013.



- 386 IPCC: Climate Change 2014: Impacts, Adaptation, and Vulnerability. Part A: Global and Sectoral Aspects. Contribution of  
387 Working Group II to the Fifth Assessment Report of the Intergovernmental Panel on Climate Change, Cambridge  
388 University Press, Cambridge, UK., 2014.
- 389 Kabat, P., Fresco, L. O., Stive, M. J. F., Veerman, C. P., van Alphen, J. S. L. J., Parmet, B. W. A. H., Hazeleger, W. and  
390 Katsman, C. A.: Dutch coasts in transition, *Nat. Geosci.*, 2(7), 450–452, doi:10.1038/ngeo572, 2009.
- 391 Kim, Y. and Newman, G.: Advancing scenario planning through integrating urban growth prediction with future flood risk  
392 models, *Comput. Environ. Urban Syst.*, 82, 101498, doi:https://doi.org/10.1016/j.compenvurbsys.2020.101498, 2020.
- 393 Kopp, R. E., DeConto, R. M., Bader, D. A., Hay, C. C., Horton, R. M., Kulp, S., Oppenheimer, M., Pollard, D. and Strauss,  
394 B. H.: Evolving understanding of Antarctic ice-sheet physics and ambiguity in probabilistic sea-level projections, arXiv,  
395 2017.
- 396 Lai, C., Shao, Q., Chen, X., Wang, Z., Zhou, X., Yang, B. and Zhang, L.: Flood risk zoning using a rule mining based on ant  
397 colony algorithm, *J. Hydrol.*, 542, 268–280, doi:https://doi.org/10.1016/j.jhydrol.2016.09.003, 2016.
- 398 Liang, X., Liu, X., Li, X., Chen, Y., Tian, H. and Yao, Y.: Delineating multi-scenario urban growth boundaries with a CA-  
399 based FLUS model and morphological method, *Landsc. Urban Plan.*, 177, 47–63,  
400 doi:10.1016/j.landurbplan.2018.04.016, 2018.
- 401 Lin, W., Sun, Y., Nijhuis, S. and Wang, Z.: Scenario-based flood risk assessment for urbanizing deltas using future land-use  
402 simulation (FLUS): Guangzhou Metropolitan Area as a case study, *Sci. Total Environ.*, 739, 139899,  
403 doi:10.1016/j.scitotenv.2020.139899, 2020.
- 404 Liu, J., Kuang, W., Zhang, Z., Xu, X., Qin, Y., Ning, J., Zhou, W., Zhang, S., Li, R., Yan, C., Wu, S., Shi, X., Jiang, N., Yu,  
405 D., Pan, X. and Chi, W.: Spatiotemporal characteristics, patterns and causes of land use changes in China since the late  
406 1980s, *Dili Xuebao/Acta Geogr. Sin.*, 69(1), 3–14, doi:10.11821/dlxb201401001, 2014.
- 407 Liu, X., Liang, X., Li, X., Xu, X., Ou, J., Chen, Y., Li, S., Wang, S. and Pei, F.: A future land use simulation model (FLUS)  
408 for simulating multiple land use scenarios by coupling human and natural effects, *Landsc. Urban Plan.*, 168, 94–116,  
409 doi:10.1016/j.landurbplan.2017.09.019, 2017.
- 410 Long, Y. and Wu, K.: Shrinking cities in a rapidly urbanizing China, *Environ. Plan. A*, 48(2), 220–222,  
411 doi:10.1177/0308518X15621631, 2016.
- 412 Muis, S., Güneralp, B., Jongman, B., Aerts, J. C. J. H. and Ward, P. J.: Flood risk and adaptation strategies under climate  
413 change and urban expansion: A probabilistic analysis using global data, *Sci. Total Environ.*, 538, 445–457,  
414 doi:10.1016/j.scitotenv.2015.08.068, 2015.
- 415 Muis, S., Verlaan, M., Winsemius, H. C., Aerts, J. C. J. H. and Ward, P. J.: A global reanalysis of storm surges and extreme  
416 sea levels, *Nat. Commun.*, 7, 11969, doi:10.1038/ncomms11969, 2016.
- 417 O’Loughlin, F. E., Neal, J., Schumann, G. J. P., Beighley, E. and Bates, P. D.: A LISFLOOD-FP hydraulic model of the  
418 middle reach of the Congo, *J. Hydrol.*, 580, doi:10.1016/j.jhydrol.2019.124203, 2020.



- 419 Parris, A., Bromirski, P., Burkett, V., Cayan, D., Culver, M., Hall, J., Horton, R., Knuuti, K., Moss, R., Obeysekera, J.,  
420 Sallenger, A. and Weiss, J.: Global Sea Level Rise Scenarios for the US National Climate Assessment, NOAA Tech  
421 Memo OAR CPO, 1–37, doi:https://scenarios.globalchange.gov/sites/default/files/NOAA\_SLR\_r3\_0.pdf, 2012.
- 422 Pecl, G. T., Araújo, M. B., Bell, J. D., Blanchard, J., Bonebrake, T. C., Chen, I. C., Clark, T. D., Colwell, R. K., Danielsen,  
423 F., Evengård, B., Falconi, L., Ferrier, S., Frusher, S., Garcia, R. A., Griffis, R. B., Hobday, A. J., Janion-Scheepers, C.,  
424 Jarzyna, M. A., Jennings, S., Lenoir, J., Linnetved, H. I., Martin, V. Y., McCormack, P. C., McDonald, J., Mitchell, N.  
425 J., Mustonen, T., Pandolfi, J. M., Pettorelli, N., Popova, E., Robinson, S. A., Scheffers, B. R., Shaw, J. D., Sorte, C. J.  
426 B., Strugnell, J. M., Sunday, J. M., Tuanmu, M. N., Vergés, A., Villanueva, C., Wernberg, T., Wapstra, E. and Williams,  
427 S. E.: Biodiversity redistribution under climate change: Impacts on ecosystems and human well-being, *Science* (80-. ),  
428 355(6332), doi:10.1126/science.aai9214, 2017.
- 429 Ramaswami, A., Russell, A. G., Culligan, P. J., Rahul Sharma, K. and Kumar, E.: Meta-principles for developing smart,  
430 sustainable, and healthy cities, *Science* (80-. ), 352, 940–943, doi:10.1126/science.aaf7160, 2016.
- 431 Reckien, D., Salvia, M., Heidrich, O., Church, J. M., Pietrapertosa, F., De Gregorio-Hurtado, S., D’Alonzo, V., Foley, A.,  
432 Simoes, S. G., Krkoška Lorencová, E., Orru, H., Orru, K., Wejs, A., Flacke, J., Olazabal, M., Geneletti, D., Feliu, E.,  
433 Vasilie, S., Nador, C., Krook-Riekkola, A., Matosović, M., Fokaidis, P. A., Ioannou, B. I., Flamos, A., Spyridaki, N. A.,  
434 Balzan, M. V., Fülöp, O., Paspaldzhiev, I., Grafakos, S. and Dawson, R.: How are cities planning to respond to climate  
435 change? Assessment of local climate plans from 885 cities in the EU-28, *J. Clean. Prod.*, 191, 207–219,  
436 doi:10.1016/j.jclepro.2018.03.220, 2018.
- 437 Song, J., Fu, X., Wang, R., Peng, Z.-R. and Gu, Z.: Does planned retreat matter? Investigating land use change under the  
438 impacts of flooding induced by sea level rise, *Mitig. Adapt. Strateg. Glob. Chang.*, 23(5), 703–733,  
439 doi:10.1007/s11027-017-9756-x, 2018.
- 440 Sosa, J., Sampson, C., Smith, A., Neal, J. and Bates, P.: A toolbox to quickly prepare flood inundation models for  
441 LISFLOOD-FP simulations, *Environ. Model. Softw.*, 123, 104561, doi:https://doi.org/10.1016/j.envsoft.2019.104561,  
442 2020.
- 443 Sun, L., Chen, J., Li, Q. and Huang, D.: Dramatic uneven urbanization of large cities throughout the world in recent decades,  
444 *Nat. Commun.*, 11(1), 5366, doi:10.1038/s41467-020-19158-1, 2020.
- 445 Tessler, Z. D., Vorosmarty, C. J., Grossberg, M., Gladkova, I., Aizenman, H., Syvitski, J. P. M. and Foufoula-Georgiou, E.:  
446 Profiling risk and sustainability in coastal deltas of the world, *Science* (80-. ), 349, 638–643,  
447 doi:10.1126/science.aab3574, 2015.
- 448 United Nations: Factsheet: People and oceans., 2017a.
- 449 United Nations: World population prospects., 2017b.
- 450 Voudoukas, M. I., Mentaschi, L., Voukouvalas, E., Verlaan, M., Jevrejeva, S., Jackson, L. P. and Feyen, L.: Global  
451 probabilistic projections of extreme sea levels show intensification of coastal flood hazard, *Nat. Commun.*, 9(1), 1–12,  
452 doi:10.1038/s41467-018-04692-w, 2018.



- 453 Wang, Z., Lai, C., Chen, X., Yang, B., Zhao, S. and Bai, X.: Flood hazard risk assessment model based on random forest, *J.*  
454 *Hydrol.*, 527, 1130–1141, doi:10.1016/j.jhydrol.2015.06.008, 2015.
- 455 Wing, O. E. J., Sampson, C. C., Bates, P. D., Quinn, N., Smith, A. M. and Neal, J. C.: A flood inundation forecast of  
456 Hurricane Harvey using a continental-scale 2D hydrodynamic model, *J. Hydrol. X*, 4, 100039,  
457 doi:https://doi.org/10.1016/j.hydroa.2019.100039, 2019.
- 458 Xian, S., Yin, J., Lin, N. and Oppenheimer, M.: Influence of risk factors and past events on flood resilience in coastal  
459 megacities: Comparative analysis of NYC and Shanghai, *Sci. Total Environ.*, 610–611, 1251–1261,  
460 doi:10.1016/j.scitotenv.2017.07.229, 2018.
- 461 Xu, K., Fang, J., Fang, Y., Sun, Q., Wu, C. and Liu, M.: The importance of digital elevation models selection in flood  
462 simulation and a proposed method to reduce DEM errors: a case study in Shanghai, *Int. J. Disaster Risk Sci.*, (in press),  
463 2021.
- 464 Xu, W. (Ato) and Yang, L.: Evaluating the urban land use plan with transit accessibility, *Sustain. Cities Soc.*, 45, 474–485,  
465 doi:10.1016/j.scs.2018.11.042, 2019.
- 466 Xu, X., Liu, J., Zhang, Z., Zhou, W., Zhang, S., Li, R., Yan, C., Wu, S. and Shi, X.: A Time Series Land Ecosystem  
467 Classification Dataset of China in Five-Year Increments (1990–2010), *J. Glob. Chang. Data Discov.*, 1(1), 52–59,  
468 doi:10.3974/geodp.2017.01.08, 2017.
- 469 Yin, J., Yu, D., Yin, Z., Wang, J. and Xu, S.: Modelling the combined impacts of sea-level rise and land subsidence on storm  
470 tides induced flooding of the Huangpu River in Shanghai, China, *Clim. Change*, 119(3–4), 919–932,  
471 doi:10.1007/s10584-013-0749-9, 2013.
- 472 Yin, J., Jonkman, S., Lin, N., Yu, D., Aerts, J., Wilby, R., Pan, M., Wood, E., Bricker, J., Ke, Q., Zeng, Z., Zhao, Q., Ge, J.  
473 and Wang, J.: Flood Risks in Sinking Delta Cities: Time for a Reevaluation?, *Earth’s Futur.*, 8(8),  
474 doi:10.1029/2020EF001614, 2020.
- 475 Zhai, Y., Yao, Y., Guan, Q., Liang, X., Li, X., Pan, Y., Yue, H., Yuan, Z. and Zhou, J.: Simulating urban land use change by  
476 integrating a convolutional neural network with vector-based cellular automata, *Int. J. Geogr. Inf. Sci.*, 34(7), 1475–  
477 1499, doi:10.1080/13658816.2020.1711915, 2020.
- 478 Zhao, L., Song, J. and Peng, Z.-R.: Modeling Land-Use Change and Population Relocation Dynamics in Response to  
479 Different Sea Level Rise Scenarios: Case Study in Bay County, Florida, *J. Urban Plan. Dev.*, 143(3), 04017012,  
480 doi:10.1061/(asce)up.1943-5444.0000398, 2017.
- 481 Zhou, L., Dang, X., Sun, Q. and Wang, S.: Multi-scenario simulation of urban land change in Shanghai by random forest and  
482 CA-Markov model, *Sustain. Cities Soc.*, 55, 102045, doi:10.1016/j.scs.2020.102045, 2020.
- 483 Zhou, Q., Leng, G., Su, J. and Ren, Y.: Comparison of urbanization and climate change impacts on urban flood volumes:  
484 Importance of urban planning and drainage adaptation, *Sci. Total Environ.*, 658, 24–33,  
485 doi:https://doi.org/10.1016/j.scitotenv.2018.12.184, 2019.



- 486 Xu, X.: China GDP Spatial Distribution Kilometer Grid Dataset [dataset], <http://www.resdc.cn/DOI/doi.aspx?DOIid=33>,  
487 2017a.
- 488 Xu, X.: China Population Spatial Distribution Kilometer Grid Dataset [dataset],  
489 <http://www.resdc.cn/DOI/DOI.aspx?DOIid=32>, 2017b.